Molecular Plant Pathology

MOLECULAR PLANT PATHOLOGY (2014) 15(3), 242–254 DOI: 10.1111/mpp.12081

Quantitative transcriptional changes associated with chlorosis severity in mosaic leaves of tobacco plants infected with *Cucumber mosaic virus*

TOMOFUMI MOCHIZUKI*, YOSHIYUKI OGATA, YUKI HIRATA AND SATOSHI T. OHKI

Graduate School of Life and Environmental Sciences, Osaka Prefecture University, Osaka 599-8531, Japan

SUMMARY

Cucumber mosaic virus (CMV) causes mosaic disease in inoculated tobacco plants. Coat protein (CP) is one of the major virulence determinants of CMV, and an amino acid substitution at residue 129 in CP alters the severity of chlorosis, such as pale green chlorosis and white chlorosis, in symptomatic tissues of mosaic leaves of infected tobacco. In this study, we compared the transcriptomes of chlorotic tissues infected with the wild-type pepo strain of CMV and two strains carrying CP mutants with diverse chlorosis severity. Differential gene expression analysis showed that CMV inoculation appeared to have similar effects on the transcriptional expression profiles of the symptomatic chlorotic tissues, and only the magnitude of expression differed among the different CMVs. Gene ontology analysis with biological process and cellular component terms revealed that many nuclear genes related to abiotic stress responses, including responses to cadmium, heat, cold and salt, were up-regulated, whereas chloroplast- and photosynthesis-related genes (CPRGs) were down-regulated, in the chlorotic tissues. Interestingly, the level of CPRG down-regulation was correlated with the severity of chlorosis. These results indicate that CP mutation governs the repression level and mRNA accumulation of CPRGs, which are closely associated with the induction of chlorosis.

INTRODUCTION

Cucumber mosaic virus (CMV) of the genus *Cucumovirus*, family *Bromoviridae*, is a major plant virus (Scholthof *et al*., 2011). CMV infects more than 1200 species in more than 100 plant families, both monocots and dicots, and causes variable disease symptoms, including leaf mosaic, stunting, chlorosis, necrosis, dwarfing and leaf malformation. Although the expression of disease symptoms depends on the host species–CMV strain specificities, one of the characteristic symptoms of CMV is a mosaic pattern on plants, which is also a characteristic viral disease symptom. On CMV infection, tobacco plants with mosaic disease show symptomatic tissues and dark green islands intermingled within uninoculated systemic leaves. Symptomatic tissues contain high levels of CMV and show chlorosis, whereas CMV infection is inhibited in dark green islands that are normal in appearance (Loebenstein *et al*., 1977).

CMV encodes at least five proteins (reviewed in Palukaitis and García-Arenal, 2003). The 1a and 2a proteins are viral RNA replication proteins. The 2b protein acts as a viral suppressor for RNA silencing (Brigneti *et al*., 1998) and also inhibits plant hormone-mediated signalling, such as salicylic acid (SA) (Ji and Ding, 2001), jasmonic acid (JA) (Lewsey *et al*., 2010) and abscisic acid (ABA) signalling (Westwood *et al*., 2013). The 3a protein is a cell-to-cell movement protein, and the coat protein (CP) is a viral structural protein that facilitates cell-to-cell and long-distance movement. CP is a virulence factor for CMV in many host plants (reviewed in Mochizuki and Ohki, 2012). Amino acid mutations in CP alter the symptomatic phenotypes in tobacco plants (Liu *et al*., 2002; Shintaku *et al*., 1992; Sugiyama *et al*., 2000; Suzuki *et al*., 1995; Szilassy *et al*., 1999; Takahashi *et al*., 2000; Yoon *et al*., 2011). In particular, the amino acid at residue 129, which is located at the first position of the βE–αEF loop of the CP molecule and regulates the flexibility of the βE–αEF loop (Gellért *et al*., 2006; Salánki *et al*., 2011), determines the severity of chlorosis in mosaic leaves of CMV-infected tobacco plants (Shintaku *et al*., 1992; Suzuki *et al*., 1995; Yoon *et al*., 2011). We have reported previously that CP mutants of the CMV pepo strain (subgroup I), in which the P at residue 129 in CP is substituted with either C, S or Q, cause severe white chlorosis in tobacco leaves, whereas substitution with either A, D or E does not alter the pale green chlorosis phenotype (Mochizuki and Ohki, 2011). Interestingly, abnormal thylakoid membranes, specifically reduced granum stacks, occur in the cells of chlorotic tissues infected with either pepo or CP mutants, with the degree of thylakoid membrane abnormality correlating with chlorosis severity; thylakoid membranes in the cells with white chlorosis mutants (129C, 129S and 129Q) are much fewer than those with pepo and pale green chlorosis mutants (129A, 129D and 129E). On the basis of this evidence, the CMV CP might determine the degree of thylakoid membrane abnormality.

**Correspondence*: Email: tomochi@plant.osakafu-u.ac.jp

© 2013 BSPP AND JOHN WILEY & SONS LTD

However, the mechanisms by which these CMV mutants influence chloroplasts remain unknown.

Microarray-based transcriptomics has commonly been used to study global comprehensive changes in host gene expression during plant–virus infections (Babu *et al*., 2008; Dardick, 2007; Jia *et al*., 2012; Rodrigo *et al*., 2012; Satoh *et al*., 2010, 2011; Senthil *et al*., 2005; Whitham *et al*., 2003). Recently, next-generation deep sequencing-based transcriptomics has also been applied to CMV-infected tobacco plants (Lu *et al*., 2012). By corresponding with pathological and physiological changes in the host plant, transcriptomics also allows for the discrimination of the specific metabolic changes that are closely associated with symptom expression (Hanssen *et al*., 2011; Rizza *et al*., 2012; Shimizu *et al*., 2007). In this study, we conducted comparative transcriptomics between the pepo strain and its CP mutants (CMVs) with varying chlorosis severity to clarify the gene expression differences among CMVs, which may allow us to identify the specific genes that are associated with abnormal thylakoid membranes and chlorosis induction. The transcriptional expression profiles in the symptomatic chlorotic tissues were qualitatively similar, but the gene expression levels were qualitatively different among the different CMVs. We found that chloroplast- and photosynthesis-related genes (CPRGs) were down-regulated in the chlorotic tissues and that the degree of down-regulation was closely correlated with the severity of chlorosis. The specific gene expression profiles associated with chlorosis are discussed.

RESULTS

Symptoms of CMV pepo and its CP mutants on tobacco plants

When the largest leaf of the five-leaf stage of tobacco plants was mechanically inoculated with pepo or its CP mutants (129A, 129C, 129D, 129E, 129Q and 129S), in which the P at residue 129 in CP was substituted, the newly developing uninoculated leaves consistently showed clear mosaic symptomatic tissue and dark green islands intermingled within a leaf at 12 days post-inoculation (dpi). Symptomatic tissues of pepo-, 129A-, 129D- and 129E-infected tobacco displayed pale green chlorosis, whereas 129C, 129Q and 129S induced severe white chlorosis (Fig. 1a). To reveal how the symptomatic chlorotic tissues developed in the CMV-infected mosaic leaves and why the chlorosis severity differed among pepo and its CP mutants (CMVs), comparative transcriptomics was conducted in the chlorotic tissues of the mosaic leaves. The distinct chlorotic tissues in the mosaic leaves

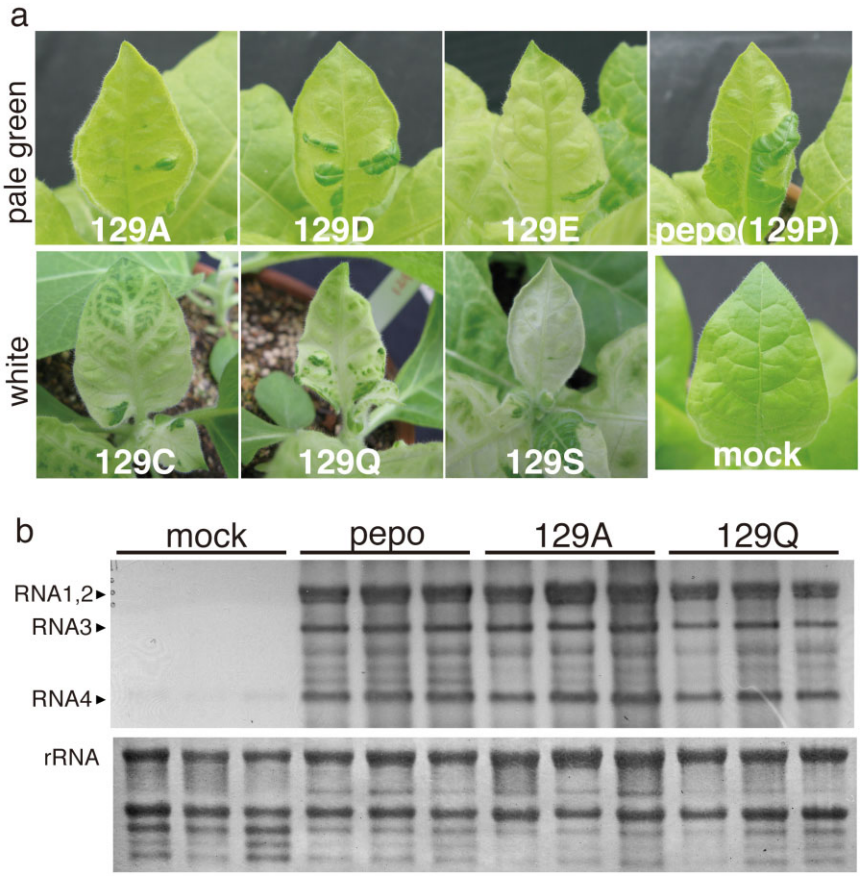

Fig. 1 (a) Symptoms of tobacco plants (*Nicotiana tabacum* cv. Samsun) inoculated with either the *Cucumber mosaic virus* pepo or one of the coat protein (CP) mutants, in which the P at residue 129 in the CP was substituted with A, C, D, E, Q or S. The photographs were obtained at 12 days post-inoculation. (b) Accumulation of *Cucumber mosaic virus* (CMV) RNA in chlorotic tissues infected with pepo, 129A, 129Q or buffer (mock). The CMV RNA amount was analysed using the total RNA samples from the microarray analysis. CMV RNA was detected by Northern blot analysis using the 3'-untranslated region (3'-UTR) of a viral genome-specific probe.

(~5 cm) at 12 dpi were collected from the individual tobacco plants inoculated with representative CMVs (pepo, 129A and 129Q). Healthy tissues from corresponding leaves of mock-inoculated tobacco plants were also sampled. It should be noted that the viral RNA titre was similar among CMVs, regardless of chlorosis severity (Fig. 1b). At least four individual tobacco plants were included per experimental group, and three biological replicates were prepared for each CMV and mock using tobacco 44K Agilent microarray analysis (Agilent Technologies, Palo Alto, CA, USA) with one-colour protocol. The outputs of the microarray in this study have been deposited in the National Center for Biotechnology Information Gene Expression Omnibus (NCBI GEO) database (series no. GSE47410) (Barrett *et al*., 2007).

Identification of differentially expressed genes (DEGs) between the mock samples and the pepo, 129A and 129Q samples

The DEGs were selected by comparison of the one-colour microarray data between mock samples and individual CMV samples. One-way analysis of variance (ANOVA) tests, followed by Tukey's *post-hoc* tests, were applied using normalized $\log_2$ intensity data. When both the ANOVA and Tukey *P* values were 0.05 or less, the gene was considered to be a DEG. In addition, DEGs showed at least a twofold average difference between the mock and CMV samples. The numbers of up-regulated genes in the pepo, 129A and 129Q samples were 1467, 1464 and 3735, respectively, and the numbers of down-regulated genes in the pepo, 129A and 129Q samples were 547, 704 and 3562, respectively. The DEGs of individual CMV samples are listed in Tables S1–S6 (see Supporting Information).

To determine which genes showed consistent expression changes in all three CMV samples, a further comparison was conducted. In this comparison, all three CMV samples (pepo, 129A and 129Q) were used as one merged test group and were collectively compared with the mock-inoculated samples using Student's *t*-test. Corrected *P* values of 0.01 or less (using a Benjamini–Hochberg multiple test correction) were used to select DEGs to obtain candidates with similar expression profiles in all three CMV samples. Genes with adjusted *P* values of 0.01 or less and at least a twofold change were considered to be DEGs. By this comparison, we identified 935 up-regulated and 225 down-regulated genes common to all three CMV samples.

Cross-comparative analysis for the identification of DEGs among the pepo, 129A and 129Q samples

A cross-comparative data analysis was used to determine which DEGs responded in similar or different ways between individual CMV samples. The cross-comparative data analysis was performed using the DEGs of individual CMV samples based on the ANOVA statistics with the *post-hoc* tests. A considerable number of identical DEGs were identified, but not all of these DEGs were identified by Student's *t*-test, in which pepo, 129A and 129Q samples were used as one merged group to obtain a more stringent selection criterion (adjusted *P* value of 0.01 or less). To broadly identify the identical DEGs that appeared to change in the same direction, i.e. that were consistently up- or down-regulated in all CMVs, but at different magnitudes, the identical DEGs obtained from both the cross-comparative data analysis using the ANOVA statistics with *post-hoc* tests and from Student's *t*-test were combined. For this strategy, we identified the identical DEGs (1058 up-regulated and 316 down-regulated) common to all three CMV samples.

Venn diagrams were used to show the number of overlapping DEGs identified in comparisons between the CMV samples (Fig. 2a,b). Interestingly, no DEGs were observed that were down-regulated in one CMV sample but up-regulated in the other two CMV samples. Thus, all DEGs of the individual CMV samples changed their expression level in the same direction, although a considerable number of genes were specifically changed in the 129Q-infected white chlorosis tissues (1056 up-regulated and 2706 down-regulated genes). Comprehensive heatmap images of the average differences in the CMV samples relative to mock samples are shown in Fig. 2c,d. Identical DEGs in all three CMV samples were hierarchically clustered using Euclidean distances. In conclusion, the CMV inoculations appeared to have similar effects on the transcriptional expression profiles in the chlorotic tissues of tobacco plants, and only the magnitude of expression differed among the CMVs.

The expression tendency of 10 representative genes [*elongation factor 1-α* (*EF1-α*), *salicylic acid-induced protein kinase* (*SIPK*), *wound-induced protein kinase* (*WIPK*), *enhanced disease susceptibility 1* (*EDS1*), *cyclin D3* (*CYCD3*), *gibberellin 20-oxidase* (*GA20ox*), *protochlorophyllide oxidoreductase 1* (*POR1*), *RNA-dependent RNA polymerase 6* (*RDR6*), *catalase 1* (*CAT1*) and *magnesium-protoporphyrin IX methyltransferase* (*CHLM*)] was confirmed by quantitative real-time reverse transcription-polymerase chain reaction (RT-qPCR) using the total RNA samples that had been used previously for the microarray analysis. Differences between the microarray analysis and the RT-qPCR analysis were observed only in *RDR6*, but the expression tendencies of the other genes obtained by RT-qPCR were similar to the results obtained by the microarray analysis (Fig. 3).

Classification of DEGs

To further deduce the host cellular components and biological processes that are affected by CMV infection, the tobacco genes (40 426 genes) from the Agilent microarray were annotated with gene ontology (GO) terms using homology searches with the data available in public databases by the BLAST program. By identifying tobacco genes with significant similarity ($<1e^{-5}$), 60.4% (24 425 genes) and 58.6% (23 707 genes) of the tobacco genes were

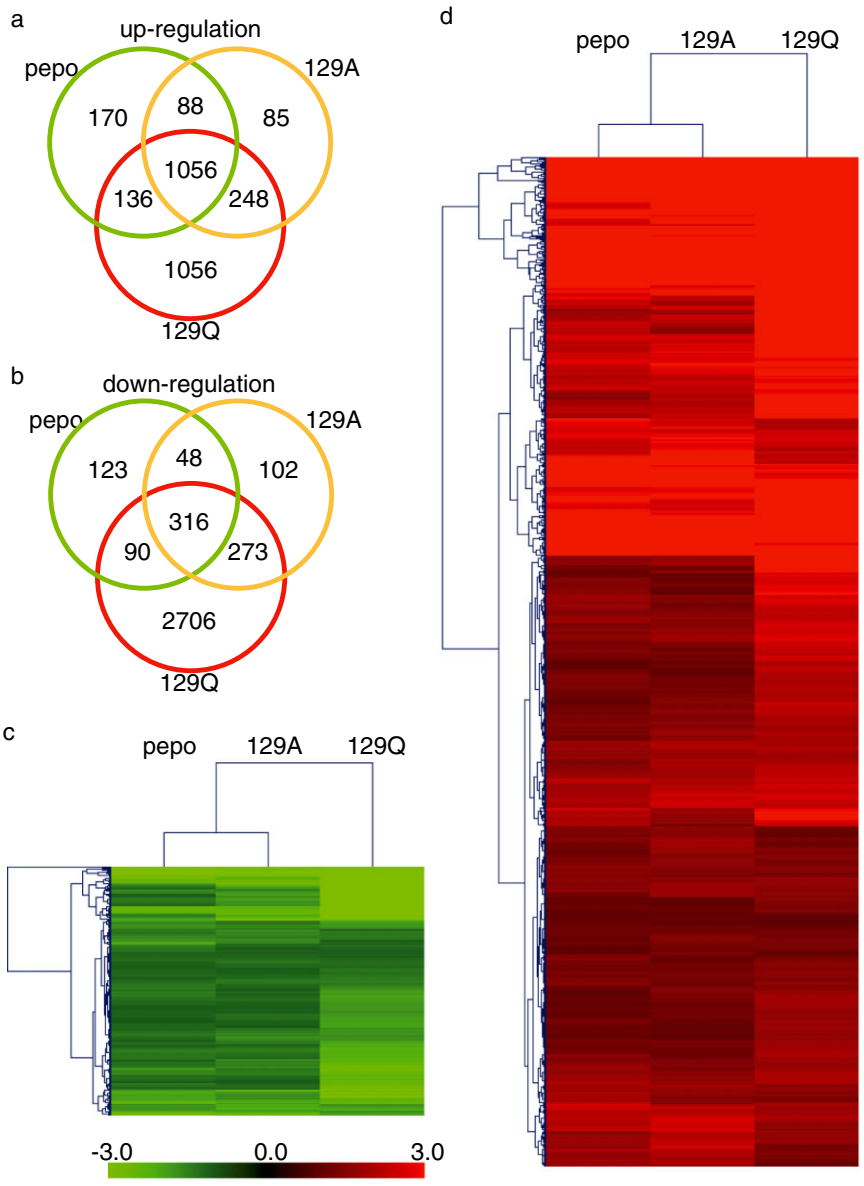

Fig. 2 (a, b) Number of specific and common differentially expressed genes (DEGs) among pepo, 129A and 129Q samples. Up-regulated and down-regulated DEGS shown in (a) and (b), respectively. (c, d) Hierarchical heat map of up-regulated (c) and down-regulated (d) identical DEGs in all three *Cucumber mosaic virus* (CMV) samples show in (a) and (b), respectively.

annotated with the cellular component and biological process aspects of GO terms, respectively. Figure 4 shows the number of identical DEGs in all three CMV samples that were annotated with cellular component terms. The top 12 biological process terms in the identical up- or down-regulated DEGs in all three CMV samples are shown in Table 1. The numbers of individual and identical DEGs that were annotated with biological process terms in the CMV samples are shown in Tables S7 and S8, respectively (see Supporting Information).

Among the up-regulated identical DEGs with cellular component terms (Fig. 4a), approximately 30% were associated with the nucleus. The cytoplasm- and plasma membrane-associated genes comprised approximately 10% of all identical DEGs, and the chloroplast- and extracellular region-associated genes comprised approximately 7%. Statistical analysis showed that the expression of genes annotated with 10 cellular component terms was enriched (Fig. 4a, asterisks). Classification of the up-regulated identical DEGs using the biological process terms (Tables 1 and S8) showed that many of the genes involved in the responses to abiotic, biotic and oxidation/toxin stresses, protein phosphorylation and transcriptional regulation were up-regulated. Approximately 35% of the down-regulated identical DEGs with cellular component terms (Fig. 4b) were associated with the chloroplast. The nucleus- and plasma membrane-associated genes comprised approximately 18% of the DEGs, and the extracellular region-associated genes comprised approximately 10% of the identical DEGs. Down-regulation of the genes annotated with 11 cellular component terms was statistically enriched, and gene

a

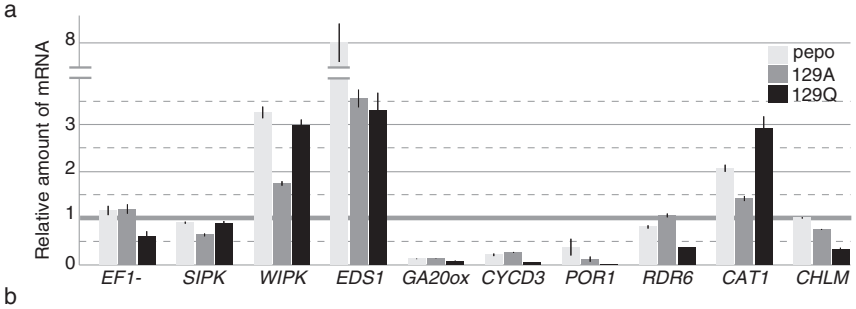

b

	EF1-	*SIPK*	*WIPK*	*EDS1*	*GA20ox*	*CYCD3*	*POR1*	*RDR6*	*CAT1*	*CHLM*
pepo	1.13	1.07	3.26	5.80	0.07	0.37	0.49	2.03	1.34	0.74
129A	1.50	1.10	2.47	4.60	0.10	0.30	0.31	1.86	1.27	0.66
129Q	1.75	1.41	4.67	4.08	0.04	0.12	0.10	1.08	4.41	0.39

Fig. 3 Validation of microarray analysis by quantitative real-time reverse transcription-polymerase chain reaction (RT-qPCR). (a) Relative amounts of representative genes (*EF1-α*, *SIPK*, *WIPK*, *EDS1*, *CYCD3*, *GA20ox*, *POR1*, *RDR6*, *CAT1* and *CHLM*) in the pepo, 129A and 129Q samples analysed by RT-qPCR. Coloured boxes indicate the relative amount of mRNA of each gene, and the bars on the boxes indicate the standard deviation among three biological replicates. mRNA amounts of each gene in the mock samples are set to unity. Total RNA samples used for the microarray analysis were also used for RT-qPCR. Serial diluted total RNAs from mock samples were used as standard quantitative controls. A random N6 primer was used for cDNA synthesis. Primers for qPCR are listed in Table S11. (b) Relative amounts of representative genes in pepo, 129A and 129Q samples calculated from the fold changes obtained by microarray analysis.

expression of five cellular component terms associated with the chloroplast was statistically significantly enriched (Fig. 4b). Classification by biological process terms showed that many genes that participated in post-translational protein modification, ethylene signalling, photosynthesis and seed development were down-regulated (Tables 1 and S8).

Distinct differences in the expression levels of DEGs between the pale green chlorosis mutants (pepo and 129A) and the white chlorosis mutant (129Q) were found in the photosynthesis and antioxidant response genes. The fold changes of representative genes are shown in Tables 2 and 3, and the gene descriptions in these tables are from Agilent's information for the tobacco microarray. Importantly, the expression levels of the genes involved in photosynthesis [chlorophyll synthesis enzymes, antenna protein (light-harvesting chlorophyll *a*/*b*-binding protein), photosystem I (PSI) and photosystem II (PSII) proteins and ribulose-1,5-bisphosphate carboxylase/oxygenase (rubisco) proteins] were much lower in the 129Q-infected white chlorosis tissues than in the pepo- and 129A-infected pale green chlorosis tissues (Table 2). However, the expression levels of catalase and cytosolic CuZn-superoxide dismutase (SOD) were up-regulated only in the 129Q samples, whereas cytosolic ascorbate peroxidase (APX) was highly expressed in all three CMV samples (Table 3). The expression levels of representative genes of hormone signalling, kinase cascades and transcription factors were similar among individual CMV samples, although expression level differences were observed in some genes related to ethylene signalling and WRKY transcription factors (Tables S9 and S10, see Supporting Information).

Down-regulation of CPRG expression is correlated with chlorosis severity in symptomatic tissues of mosaic leaves

To confirm the relation between CPRG down-regulation and chlorosis, the mRNA levels of representative CPRGs in the chlorotic tissues and dark green islands of mosaic leaves of plants infected with pepo or the six CP mutants (129A, 129C, 129D, 129E, 129Q and 129S, Fig. 1a) were compared (Fig. 5). The mRNA levels of the antenna proteins (*LHCA1* and *LHCB6*), chlorophyll synthesis enzymes (*PPIX* and *CHLH*), small and large rubisco subunits (*RBC S* and *RBC L*), PSII D1 core protein (*PSB A*) and electron transport chain complex proteins (*PET A* and *PET B*) were analysed by Northern blot analysis using three individual samples for each CMV. The levels of *LHCA1*, *LHCB6* and *CHLH* were lowest in the white chlorosis mutant tissues and were lower in the pepo and pale green chlorosis mutant tissues than in the mock-inoculated tissues. The levels of *RBC S*, *RBC L*, *PSB A*, *PET A* and *PET B* were lower in the white chlorosis mutant tissues than in the pale green chlorosis mutant and mock tissues. In contrast, the levels of *PPIX* were no different among the mock, pepo, pale green mutant or white mutant tissues. These results correspond to those of the microarray analysis. It should be noted that the mRNA levels of the CPRGs in the dark green islands of the mosaic leaves inoculated with pepo or the six CP mutants were similar to those of the mock-inoculated leaves, showing that the expression level of the CPRGs was repressed only in the symptomatic tissues. These results indicate that the degree of CPRG repression is closely associated with the severity of chlorosis.

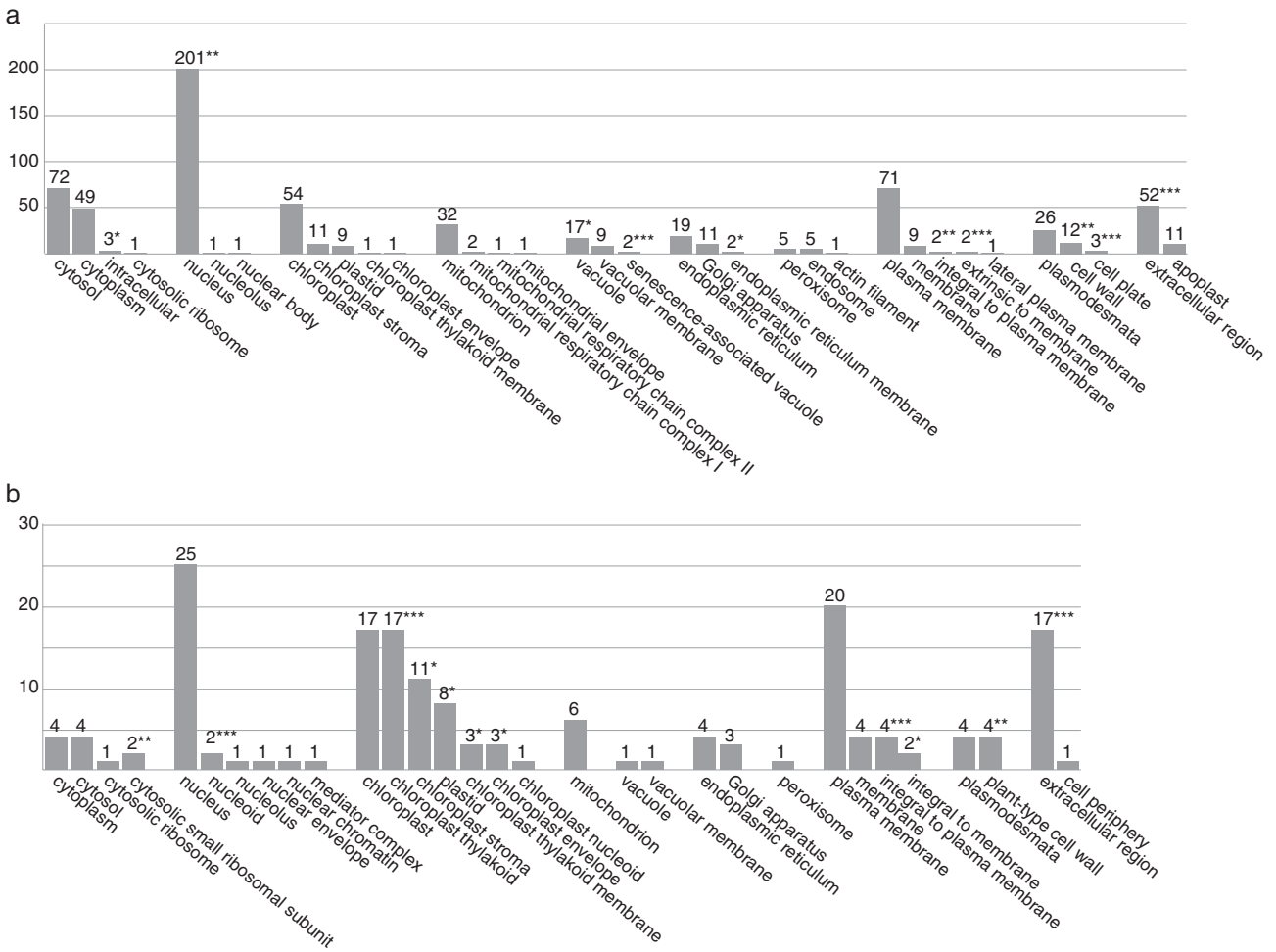

Fig. 4 Number of identical differentially expressed genes (DEGs) in all three *Cucumber mosaic virus* (CMV) samples, annotated with cellular component gene ontology (GO) terms. (a) Up-regulated identical DEGs. (b) Down-regulated identical DEGs. The *P* value for the binomial distribution was calculated based on the ratio between the percentage of identical DEGs and the percentage of background population genes in each cellular component GO term. Statistically significantly enriched GO terms are shown with an asterisk: $*P < 0.05$; $**P < 0.01$; $***P < 0.001$.

DISCUSSION

To understand the induction mechanisms of chlorosis, we compared the transcriptomes of the symptomatic chlorotic tissues of mosaic leaves infected with CMV mutants with differing chlorosis severity. Our microarray analysis revealed that CMV inoculation caused qualitatively similar transcriptional expression profiles regardless of chlorosis severity, and only quantitative differences in tobacco gene expression profiles correlated with chlorosis severity were detected among the CMVs. These results suggest that DEGs with different expression levels among the CMV samples are associated with chlorosis severity, whereas identical DEGs with similar expression levels among the CMV samples are associated with the general host response to CMV infection. Interestingly, the down-regulation of CPRGs was tightly correlated with chlorosis severity. The roles of altered gene expression levels (through CMV infection), especially in photosynthesis, and antioxidant responses that are tightly associated with chlorosis are discussed below.

Photosynthesis

The chlorotic symptoms of viral infection have been associated with the malformation of the chloroplast structure (Díaz-Vivancos *et al*., 2008; Lehto *et al*., 2003; Mochizuki and Ohki, 2011; Ohnishi *et al*., 2009). Many previous studies have shown that virus/viroid infection reduces the mRNA accumulation of CPRGs in chlorotic tissues (Babu *et al*., 2008; Dardick, 2007; Rizza *et al*., 2012; Satoh *et al*., 2010, 2011; Shimizu *et al*., 2007; Yang *et al*., 2007). Meta-analysis using *Arabidopsis* microarray data containing distinct virus infection has also indicated that the down-regulation of photosynthesis-related metabolic processes is a common response

Table 1 Top 12 biological process terms in identical up- or down-regulated differentially expressed genes (DEGs) in all three *Cucumber mosaic virus* (CMV) samples.

Biological process gene ontology term	Number of annotated genes
Up-regulated identical DEGs	
Biological_process	86
Response to cadmium ion	17
Response to cold	17
Response to heat	17
Response to salt stress	17
Protein phosphorylation	15
Response to abscisic acid stimulus	15
Regulation of transcription, DNA-dependent	14
Oxidation–reduction process	13
Metabolic process	11
Proteolysis	11
Ubiquitin-dependent protein catabolic process	11
Down-regulated identical DEGs	
Biological_process	27
Protein phosphorylation	10
Response to ethylene stimulus	9
Photosynthesis, light reaction	5
Peptidyl-cysteine *S*-nitrosylation	4
Defence response to bacterium	3
Embryo development ending in seed dormancy	3
Lipid transport	3
Photoinhibition	3
Photosynthetic electron transport in photosystem II	3
Regulation of transcription, DNA-dependent	3
Seed development	3

against viruses (Rodrigo *et al*., 2012). Lu *et al*. (2012) have shown that the CMV M strain depresses many CPRGs during the symptom development process in tobacco, suggesting that the chloroplast development and photosynthesis pathways, especially pigment metabolism, are directly responsible for symptom expression. The present study has demonstrated that the repression level of CPRGs, such as the chlorophyll synthesis enzymes and antenna proteins, is correlated with chlorosis severity and the degree of thylakoid membrane abnormality (Table 2 and Fig. 5; Mochizuki and Ohki, 2011). This novel finding strongly supports the hypothesis of Lu *et al*. (2012) that the repression of chloroplast and photosynthetic metabolism results from the repression of CPRGs on CMV infection, causing chlorosis.

Wang *et al*. (2000) have indicated that CMV infection alters the photosynthetic activity of infected tobacco via the inhibition of PSII activity. The inhibition of PSII activity and the decrease in 22-kDa and 23-kDa oxygen-evolving proteins (OEPs, PSII components) occur only in CMV-Y-infected yellow tissues, but not in CMV-O-infected asymptomatic tissues (Takahashi and Ehara, 1992; Takahashi *et al*., 1991). Our microarray analysis has shown that the expression of *OEP*s is reduced in chlorotic tissues (Table 2), suggesting that the decreased accumulation of OEPs observed by Takahashi *et al*. (1991) is caused by the repression of *OEP* mRNAs rather than by post-translational degradation. Knockdown of the 23-kDa *OEP* (*PsbP*) causes the disordering of granum stacks by the impairment of PSII super-complex accumulation (Ido *et al*., 2009; Yi *et al*., 2009). Decreased mRNA accumulation of the chlorophyll synthesis enzymes or antenna proteins also induces abnormal thylakoid membrane formation (Fitter *et al*., 2002; Luo *et al*., 2013; Waters *et al*., 2009). These findings validate the hypothesis that the decreased expression of CPRGs on CMV infection causes abnormal thylakoid membrane formation in chlorotic tissues.

Antioxidant response

Díaz-Vivancos *et al*. (2008) have reported that chloroplast structure and metabolism are altered by *Plum pox virus* infection, leading to the generation of reactive oxygen species (ROS) in the chloroplasts and alteration of antioxidant enzyme activities. Therefore, these authors suggested that chloroplasts were a source of oxidative stress. *Sunflower chlorotic mottle virus* infection also alters antioxidant enzyme activities at the gene expression level, which are associated with chlorotic symptom development (Arias *et al*., 2005; Rodríguez *et al*., 2012). In the cells of CMV-infected tomato and cucumber, especially in chloroplasts, abundant H_2O_2 accumulates and antioxidant enzyme activities are altered in the chloroplasts and mitochondria rather than in the cytoplasm (Song *et al*., 2009). We found that the expression levels of *CAT* and cytosolic *Cu/Zn-SOD* were up-regulated only in the 129Q samples of white chlorosis tissues (Table 3). The expression levels of chloroplast-related *Fe-SOD* genes were also increased slightly only in the 129Q samples (Table 3). These data indicate that these antioxidant enzyme activities are associated with chlorosis severity and the degree of thylakoid membrane abnormality (Mochizuki and Ohki, 2011). It has been speculated that the severe disorder of thylakoid membranes caused by 129Q infection induces ROS generation in chloroplasts, leading to the high expression levels of *CAT* and *Cu/Zn-SOD*. However, *CAT* and *Cu/Zn-SOD* are mainly localized to the peroxisomes and cytoplasm rather than the chloroplasts. In addition, the expression levels of chloroplast-related antioxidant genes (e.g. thylakoid-bound *APX* and *Fe-SOD*) are almost unaltered in the 129Q samples (Table 3). Thus, there also remains the possibility that 129Q infection induces oxidative stress in the cytoplasm independent of the thylakoid membrane disorder.

In the pepo and 129A samples, the expression levels of antioxidant genes, except for cytosolic *APX*, were almost unaltered. Thus, in the pale green chlorosis tissues, oxidative stress might have been removed sufficiently by the antioxidative enzyme activities that occur at normal expression levels or ROS might not have been generated in abnormal chloroplasts because the photosynthetic activity was depressed by the down-regulation of CPRGs. García-Marcos *et al*. (2009) have speculated that the oxidative

 © 2013 BSPP AND JOHN WILEY & SONS LTD

Table 2 Gene responses to photosynthesis by *Cucumber mosaic virus* (CMV) infections.

Seq_ID	Gene_ID	Description*	Fold change		
			pepo	129A	129Q
Chlorophyll synthesis enzymes					
2063895	AM746200	gb|*Nicotiana tabacum* partial mRNA for glutamyl tRNA reductase (hemA gene) [AM746200]	−1.449	−1.714	−3.729
2087091	Y13465	gb|*Nicotiana tabacum* mRNA for protoporphyrin IX oxidase, ppxI gene [Y13465]	−1.348	−1.489	−2.230
2071594	Y13466	gb|*Nicotiana tabacum* mRNA for protoporphyrin IX oxidase, ppxII gene [Y13466]	−1.306	−1.478	−2.000
2056751	AF014052	gb|*Nicotiana tabacum* Mg protoporphyrin IX chelatase (Chl H) mRNA, complete cds [AF014052]	−1.812	−2.312	−4.406
2062458	AF014051	gb|*Nicotiana tabacum* Mg chelatase subunit (ChlH) mRNA, partial cds [AF014051]	−2.653	−3.811	−8.932
2053947	AF014053	gb|*Nicotiana tabacum* Mg protoporphyrin chelatase subunit (Chl I) mRNA, complete cds [AF014053]	−1.465	−1.375	−2.598
2086473	AF213968	gb|*Nicotiana tabacum S*-adenosyl-L-methionine Mg-protoporphyrin IX methyltranserase (Chl M) mRNA, complete cds; chloroplast gene for chloroplast product [AF213968]	−1.345	−1.507	−2.581
2088483	AB074570	gb|*Nicotiana tabacum* POR1 mRNA for NADPH:protochlorophyllide oxidoreductase, complete cds [AB074570]	−2.040	−3.204	−10.222
2045033	AB074571	gb|*Nicotiana tabacum* POR2 mRNA for NADPH:protochlorophyllide oxidoreductase, complete cds [AB074571]	−1.942	−2.086	−5.333
2071017	TA14106_4097	tc|Rep: NADPH:protochlorophyllide oxidoreductase—*Nicotiana tabacum* (Common tobacco), complete [TC123693]	−2.151	−3.021	−10.959
2056228	EB435437	gb|*Nicotiana tabacum* cultivar SNN chlorophyll synthase (CHLG) mRNA, CHLG-1 allele, complete cds [FJ905101]	−1.858	−1.607	−2.516
Antenna proteins					
2066778	TA12484_4097	tc|Rep: Photosystem I light-harvesting chlorophyll *a*/*b*-binding protein—*Nicotiana tabacum* (Common tobacco), complete [TC123481]	−1.279	−1.740	−5.903
2056014	DQ676843	gb|*Nicotiana tabacum* chloroplast pigment-binding protein CP29 (Lhcb4) mRNA, complete cds; nuclear gene for chloroplast product [DQ676843]	1.068	−1.079	−2.272
2046950	TA11963_4097	tc|Rep: Chloroplast pigment-binding protein CP26—*Nicotiana tabacum* (Common tobacco), complete [TC125988]	−1.189	−1.431	−2.541
2045845	TA12003_4097	tc|Rep: Chloroplast pigment-binding protein CP24—*Nicotiana tabacum* (Common tobacco), complete [TC123534]	−1.335	−2.005	−8.176
2061062	AY219853	gb|*Nicotiana tabacum* chlorophyll *a* [AY219853]	−1.465	−2.349	−7.952
2076491	EB437069	gb|Tobacco Cab40 mRNA for major chlorophyll *a* [X52744]	1.096	1.015	−2.454
2065407	TA14592_4097	tc|Rep: Light harvesting chlorophyll *a*/*b*-binding protein precursor—*Nicotiana sylvestris* (Wood tobacco), complete [TC123590]	−2.256	−3.390	−38.019
PSI-related proteins					
2066487	TA11940_4097	tc|Rep: Photosystem I reaction centre subunit X psaK—*Nicotiana tabacum* (Common tobacco), complete [TC145810]	−1.987	−2.698	−5.533
2055540	TA12233_4097	tc|Rep: Photosystem I psaH protein precursor—*Nicotiana sylvestris* (Wood tobacco), complete [TC160540]	−1.071	−1.311	−2.356
2049821	X61665	gb|*Nicotiana tabacum* psaH gene for photosystem I psaH protein [X61665]	−1.524	−1.895	−3.951
2059656	TA15345_4097	tc|Rep: PSI-D1 precursor—*Nicotiana sylvestris* (Wood tobacco), partial (98%) [TC132237]	−1.100	−1.345	−6.228
2061307	TA13529_4097	tc|Rep: Photosystem I reaction centre subunit IV A, chloroplast precursor (PSI-E A) [Contains: Photosystem I reaction centre subunit IV A isoform 2]—*Nicotiana sylvestris* (Wood tobacco), complete [TC139467]	−1.458	−1.701	−4.772
2062539	EB681816	tc|Rep: Photosystem I subunit XI—*Nicotiana attenuata*, partial (54%) [TC163205]	−2.050	−3.723	−15.889
PSII-related proteins					
2074876	EB435020	tc|Rep: Chloroplast photosystem II PsbR—*Prosopsis juliflora* (Mesquite) (Algorrobo), partial (97%) [TC136185]	1.494	2.859	1.213
2073564	TA14635_4097	tc|Rep: Photosystem II P680 chlorophyll A apoprotein—*Solanum lycopersicum* (Tomato) (*Lycopersicon esculentum*), complete [TC126534]	1.036	1.079	1.105
2065604	X55354	gb|*Nicotiana tabacum* mRNA for a photosystem II 23-kDa polypeptide [X55354]	−1.851	−2.152	−6.004
2088164	TA21687_4097	tc|Rep: Photosystem II 44-kDa reaction centre protein—*Nicotiana tabacum* (Common tobacco), partial (59%) [TC143855]	−1.017	−1.029	−1.162
2049904	AY220076	gb|*Nicotiana tabacum* oxygen-evolving complex 33-kDa photosystem II protein (PsbO) mRNA, complete cds; nuclear gene for chloroplast product [AY220076]	−1.474	−2.183	−4.278
2055573	TA11936_4097	tc|Rep: Chloroplast oxygen-evolving protein 16-kDa subunit—*Nicotiana tabacum* (Common tobacco), complete [TC126580]	1.237	−1.677	−3.939
Electric transport chain proteins					
2050723	EH621693	tc|Rep: Plastid quinol oxidase—*Solanum lycopersicum* (Tomato) (*Lycopersicon esculentum*), partial (86%) [TC141050]	−1.075	1.110	1.217
2058215	TC74155	tc|Rep: Cytochrome b6—*Nicotiana sylvestris* (Wood tobacco), partial (48%) [TC166043]	1.006	1.006	−1.315
Rubisco proteins					
2084950	TA11967_4097	tc|Rep: Ribulose bisphosphate carboxylase large chain precursor—*Nicotiana sylvestris* (Wood tobacco), complete [TC122913]	1.302	1.263	−1.029
2053317	EB435775	tc|Rep: Ribulose bisphosphate carboxylase small chain—*Nicotiana tabacum* (Common tobacco), complete [TC165446]	−1.554	−1.330	−3.268
2063791	TA11709_4097	tc|Rep: Ribulose bisphosphate carboxylase small chain, chloroplast precursor—*Nicotiana sylvestris* (Wood tobacco), complete [TC126140]	1.121	1.181	1.003
2053421	U35620	gb|*Nicotiana tabacum* ribulose-1,5 bisphosphate carboxylase [U35620]	−1.417	−1.334	−2.303
Chlorophyll catabolism					
2049008	EU294210	gb|*Nicotiana tabacum* putative chlorophyllase mRNA, complete cds [EU294210]	−1.372	−1.086	−1.875
2064248	EU294213	gb|*Nicotiana tabacum* putative red chlorophyll catabolite reductase mRNA, complete cds [EU294213]	−1.088	1.040	1.391
Chloroplast differentiation					
2046133	EF606850	gb|*Nicotiana tabacum* plastid division regulator MinD mRNA, complete cds; nuclear gene for plastid product [EF606850]	−1.544	−1.295	−1.754
2053978	AJ133453	gb|*Nicotiana tabacum* mRNA for FtsZ-like chloroplast protein [AJ133453]	−1.817	−1.589	−2.193
2052856	AJ271748	gb|*Nicotiana tabacum* partial mRNA for chloroplast FtsZ-like protein (ftsZ gene), clone FtsZ1-1 [AJ271748]	−1.509	−1.588	−2.372

*The gene descriptions are from Agilent's information for the tobacco microarray.

Table 3 Gene responses to antioxidants by *Cucumber mosaic virus* (CMV) infections.

Seq_ID	Gene_ID	Description*	Fold change		
			pepo	129A	129Q
Catalase					
2047518	U07627	gb|*Nicotiana tabacum* Petit Havana SR1 catalase (CAT-1) mRNA, complete cds [U07627]	1.715	1.862	5.573
2087798	EF532799	gb|*Nicotiana tabacum* cultivar Xanthi catalase mRNA, partial cds [EF532799]	1.340	1.267	4.408
2069710	EB432848	tc|Rep: Catalase isozyme 3—*Nicotiana plumbaginifolia* (Leadwort-leaved tobacco), partial (62%) [TC131485]	1.518	1.554	2.033
Superoxide dismutase					
2045375	DR109312	gb|HAP4-17 Cultured tobacco cells *Nicotiana tabacum* cDNA 3' similar to putative mRNA cytostolic CuZn-superoxide dismutase (cyt-SOD1 gene), mRNA sequence [DR109312]	1.333	1.561	2.396
2068264	EB442731	tc|Rep: Superoxide dismutase [Cu-Zn]—*Populus tremula* × *Populus tremuloides*, partial (96%) [TC140325]	−1.174	−1.134	−2.220
2061599	TA12140_4097	tc|Rep: Superoxide dismutase [Cu-Zn]—*Nicotiana plumbaginifolia* (Leadwort-leaved tobacco), complete [TC158847]	1.466	1.470	1.871
2055267	DW004086	tc|Rep: Superoxide dismutase [Fe]—*Solanum lycopersicum* (Tomato) (*Lycopersicon esculentum*), partial (95%) [TC133555]	−1.393	−1.008	1.762
2052338	EB430982	tc|Rep: Superoxide dismutase [Fe]—*Solanum lycopersicum* (Tomato) (*Lycopersicon esculentum*), complete [TC135414]	−1.367	1.199	1.510
2080462	EB429945	tc|Rep: Superoxide dismutase [Mn], mitochondrial precursor—*Nicotiana plumbaginifolia* (Leadwort-leaved tobacco), complete [TC123616]	−1.201	1.014	−1.196
Ascorbate/glutathione cycle					
2067007	TA11931_4097	tc|Rep: Cytosolic ascorbate peroxidase—*Nicotiana tabacum* (Common tobacco), complete [TC152466]	2.698	3.033	2.744
2068600	D85912	gb|*Nicotiana tabacum* mRNA for cytosolic ascorbate peroxidase, complete cds [D85912]	1.972	2.283	2.399
2059388	FG148935	tc|Rep: Stromal ascorbate peroxidase—*Nicotiana tabacum* (Common tobacco), partial (67%) [TC123903]	2.220	−1.237	1.255
2075790	BP535437	tc|Rep: Thylakoid-bound ascorbate peroxidase—*Nicotiana tabacum* (Common tobacco), complete [TC125928]	−1.143	1.059	−1.567
2063187	AB022273	gb|*Nicotiana tabacum* mRNA for thylakoid-bound ascorbate peroxidase, complete cds [AB022273]	−1.057	1.048	−1.386
2072727	NP917705	tc|Rep: Glutathione reductase, chloroplast precursor—*Nicotiana tabacum* (Common tobacco), complete [TC163303]	−1.291	−1.237	−1.392
2064573	X76293	gb|*Nicotiana tabacum* gor mRNA for glutathione reductase [X76293]	−1.528	−1.262	−1.410
2068132	DV160693	tc|Rep: Monodehydroascorbate reductase—*Solanum lycopersicum* (Tomato) (*Lycopersicon esculentum*), complete [TC141234]	1.044	1.245	1.270
2082901	TA12494_4097	tc|Rep: Dehydroascorbate reductase—*Nicotiana tabacum* (Common tobacco), complete [TC124291]	1.204	1.092	1.311
2084132	TA16711_4097	tc|Rep: Dehydroascorbate reductase—*Solanum tuberosum* (Potato), partial (92%) [TC149963]	−1.248	−1.146	−2.635
2054343	AY074787	gb|*Nicotiana tabacum* dehydroascorbate reductase (DHAR) mRNA, complete cds [AY074787]	−1.021	−1.046	1.157
2068260	TA14928_4097	tc|Rep: Probable monodehydroascorbate reductase, cytoplasmic isoform 2—*Arabidopsis thaliana* (Mouse-ear cress), partial (89%) [TC123260]	−1.132	−1.134	−1.392

*The gene descriptions are from Agilent's information for the tobacco microarray.

damage in the chloroplast by the synergistic effect of *Potato virus Y–Potato virus X* (PVY–PVX) mixed infection is minimized by the repression of photosynthetic metabolism. Indeed, the plant reduces its photosynthetic activity via the depression of nuclear-encoded CPRGs to reduce the oxidative stress of photoinhibition induced by high light (Waters and Langdale, 2009). When the chloroplasts are subjected to oxidative stress, repression of nuclear-encoded CPRGs is induced by chloroplast-to-nucleus retrograde signals, such as ROS derived from damaged chloroplasts (Barajas-Lopez *et al*., 2013; Galvez-Valdivieso and Mullineaux, 2010). Thus, in order to avoid the oxidative damage caused by CMV infection stress, the depression level of CPRGs might be rigorously controlled via retrograde signalling between the chloroplast and nucleus.

Why are transcriptional expression profiles different among CMV pepo and CP mutants?

One of the important questions of this study is why the chlorosis severity differed among the CMVs even though only one amino acid difference existed in residue 129 of the CP. The viral titre was similar among the CMVs (Fig. 1b), showing that amino acid 129 did not determine host gene expression via regulation of the CMV titre. Because CMV virions and CP molecules usually exist in the cytoplasm, the surface properties or structural changes of the virion or CP molecule by the amino acid substitutions at residue 129 are thought to alter the stress intensity given to a host cell in the cytoplasm, which governs the degree of CPRG expression changes. Alternatively, Liang *et al*. (1998) have reported that the

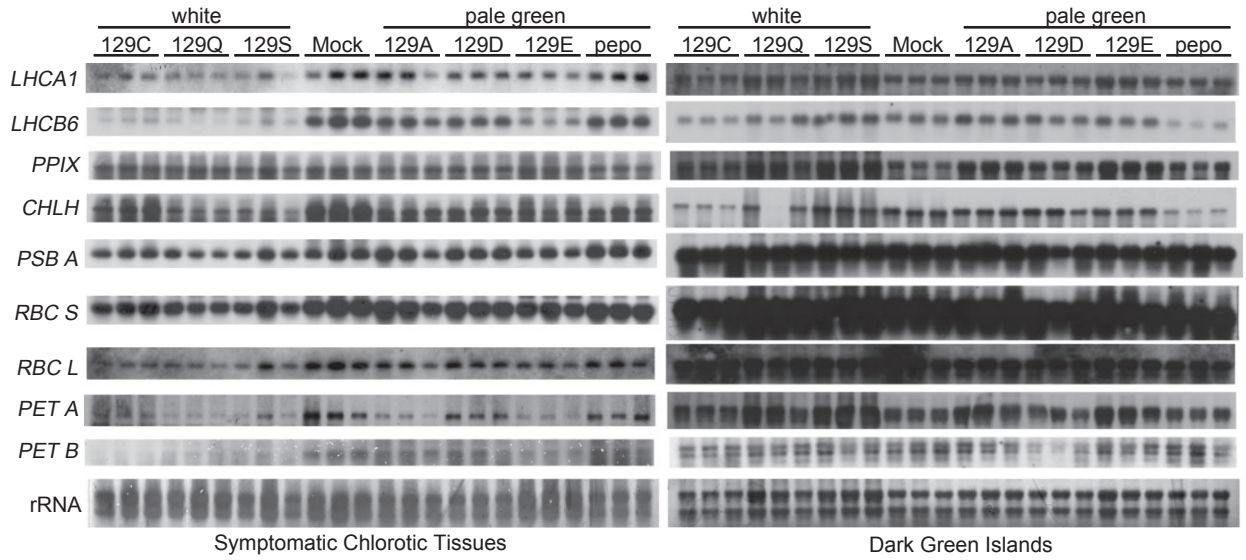

Fig. 5 Northern blot analysis of chloroplast- and photosynthesis-related genes in the total RNA extracted from the chlorotic tissues or dark green islands of mosaic leaves with either pepo or its coat protein (CP) mutants, in which the P at residue 129 in the CP was substituted by A, C, D, E, Q or S. The symptoms of each *Cucumber mosaic virus* (CMV) are shown in Fig. 1a. Three samples from three individual plants per CMV were investigated. The genes of the antenna proteins (*LHCA1* and *LHCB6*), chlorophyll synthesis enzymes (*PPIX*, *CHLH*), small and large subunits of ribulose-1,5-bisphosphate carboxylase/oxygenase (rubisco) (*RBC S*, *RBC L*), photosystem II (PSII) D1 core protein (*PSB A*) and electron transport chain complex proteins (*PET A* and *PET B*) were analysed by Northern blot analysis with digoxygenin (DIG)-labelled gene-specific RNA probes. The primers for the PCR amplification of each gene used to synthesize the RNA probes are listed in Table S12.

CMV CP molecules are transported into chloroplasts and then induce chlorosis; they have suggested that the amount of CP in the chloroplasts correlates with CMV virulence. Amino acid substitution at residue 129 by either F or L in the CP inhibits virion assembly and aggregates the CP molecules (Suzuki *et al*., 1995). Based on these reports, it is possible that CP molecules affect host gene expression regulation via chloroplast targeting, and that the 129P → C, Q and S substitutions promote chloroplast localization of the CP molecules by the repression of virion assembly. Further studies are needed to reveal how the CMV CP mutants regulate host gene expression at a quantitative level.

EXPERIMENTAL PROCEDURES

Virus, plant and inoculation

The pepo strain of CMV (pepo) [GenBank accession numbers AB124834 (RNA 1), AB124835 (RNA 2) and AF103991 (RNA 3)] and the CP mutants of pepo containing a modified CP, in which the P at residue 129 is substituted with A, C, D, E, Q or S (Mochizuki and Ohki, 2011), were used. The largest leaf of the five-leaf stage of tobacco (*Nicotiana tabacum* cv. Samsun) was mechanically inoculated with either purified virus (100 μg/mL in phosphate buffer) or phosphate buffer (mock control). For microarray analysis, at least four individual tobacco plants were used per biological replicate (mock, pepo, 129A or 129Q), and three biological replicates were prepared. The inoculated plants were grown in a growth chamber (CLE-303, TOMY Seiko, Tokyo, Japan) with a 16-h light (25 °C)/8-h dark (22 °C) cycle.

Preparation of total RNA for microarray analysis

Distinct chlorotic tissues from uninoculated mosaic leaves infected with CMVs and the corresponding upper leaves of mock-inoculated plants were sampled at 12 dpi, and leaf pieces were immediately frozen with liquid nitrogen and stored at −80 °C. Total RNA was extracted from 100-mg leaf samples using the RNeasy Plant Mini Kit with DNase I treatment (Qiagen, Valencia, CA, USA). RNA concentration and integrity were analysed with an Agilent 2100 Bioanalyzer (Agilent Technologies).

Detection of CMV RNAs

Two micrograms of total RNA were loaded onto a 1.5% denaturing agarose gel and transferred to a Biodyne Plus membrane (Pall, East Hills, NY, USA). The membrane was hybridized with digoxygenin (DIG)-labelled RNA probes complementary to the conserved 3'-untranslated region (3'-UTR) sequence (Saitoh *et al*., 1999) in the UltraHyb (Ambion, Austin, TX, USA). The detection of DIG signals was performed according to the manufacturer's instructions (Roche, Basel, Schweiz). The total RNA on the membrane was stained with methylene blue as a loading control.

Microarray analysis

Microarray analysis was conducted by Miltenyi Biotec (Bergisch Gladbach, Germany). For the linear T7-based amplification step, 100 ng of each total

RNA sample were used. To produce the cyanine-3 (Cy3)-labelled cRNA, the RNA samples were amplified and labelled using an Agilent Low Input Quick Amp Labeling Kit (Agilent Technologies) following the manufacturer's protocol. Yields of cRNA and the dye incorporation rate were measured with an ND-1000 spectrophotometer (NanoDrop Technologies, Wilmington, DE, USA).

The hybridization procedure was performed according to the Agilent 60-mer oligo microarray processing protocol using the Agilent Gene Expression Hybridization Kit (Agilent Technologies), and 1.65 μg of Cy3-labelled fragmented cRNA in hybridization buffer was hybridized overnight (17 h, 65 °C) to Agilent Whole Tobacco Genome Oligo Microarrays 4x44K. Finally, the microarrays were washed once with Agilent Gene Expression Wash Buffer 1 for 1 min at room temperature, followed by a second wash with Agilent Gene Expression Wash Buffer 2 for 1 min at 37 °C. The last washing step was performed with acetonitrile. Fluorescence signals were detected using Agilent's Microarray Scanner System (Agilent Technologies). Agilent Feature Extraction Software (FES) was used to read and process the microarray image files. The signal intensities from the single-experiment raw data were normalized by dividing the intensity values by their median.

Discriminatory gene analysis

Bioinformatic analysis was also conducted by Miltenyi Biotec. After background correction, quantile normalization was conducted between arrays. Finally, the normalized intensities were $\log_2$-transformed and served as the basis for further analysis.

We used a combination of both significance and fold-change criteria to identify biologically meaningful expression changes. In this experimental design, a one-way ANOVA test, followed by Tukey's *post-hoc* analysis, was applied using the normalized $\log_2$ intensity data. Expression differences between sample groups were considered to be significant if both the ANOVA and Tukey *P* values of the indicated comparison were 0.05 or smaller. In addition to $P \leq 0.05$, genes selected as reliable candidates were required to show at least a twofold average expression difference between the mock and sample groups.

A separate analysis was conducted in which all CMV samples were collectively used as a common test group. This collective group of all CMV samples was compared with the mock-treated samples using Student's *t*-test. The *P* values obtained from this analysis are therefore based on the probability associated with the *t*-distribution. Despite the fact that all the CMV samples were consistently up-regulated, the magnitude of the expression differences within the merged test group was relatively high, resulting in higher (not significant) *P* values that no longer met the selection criterion. Therefore, a more stringent selection criterion was applied to the *t*-tests: DEGs were considered when they had an adjusted *P* value using the Benjamini–Hochberg multiple test correction that was less than or equal to 0.01 and at least a twofold magnitude in the expression difference.

GO analysis

We obtained plant peptide sequence databases from the NCBI FTP site (ftp://ftp.ncbi.nih.gov/refseq/release/plant/). To associate the plant peptide sequences with the GO terms assigned to *Arabidopsis* genes, we performed a BLAST search, in which queries were the plant peptide sequences and subjects were the *Arabidopsis* peptide sequences obtained from The *Arabidopsis* Information Resource (TAIR) database (http://www.arabidopsis.org/). Then, the plant peptide sequences hit to the *Arabidopsis* peptide sequences were selected as a sequence database for the search of GO terms in plants; the database is available at our website (http://www.plant.osakafu-u.ac.jp/~ogata/downloadgo.html). The original sequences of tobacco genes of 60-mer DNA probes on Agilent's microarray were compared with the selected sequence database, and GO terms included in the aspects of cellular component and biological process were assigned to the probes based on the significant similarity ($<1e^{-5}$). To statistically identify the significantly enriched cellular component GO terms of the DEGs, the *P* value for the binomial distribution was calculated based on the ratio between the percentage of identical DEGs and the percentage of background population genes in each cellular component GO term.

Validation of microarray analysis by RT-qPCR

To validate the microarray analysis, RT-qPCR was performed. The total RNA samples used for the microarray analysis were applied for RT-qPCR. Serial diluted total RNA from mock samples was used as a standard quantitative control. cDNA was synthesized from 1 μg of total RNA using ReverTra Ace (Toyobo, Osaka, Japan) with a random N6 primer. The nucleotide sequences of *EF1-α*, *EDS1*, *CYCD3*, *GA20ox*, *CAT1* and *CHLM* were obtained from the NCBI database, and specific primer sets were designed using the Primer3 Plus program (http://www.bioinformatics.nl/cgi-bin/primer3plus/primer3plus.cgi) (Table S11, see Supporting Information). The primer sequences for *RDR6*, *POR1*, *SIPK*, *WIPK* and actin were taken from previous reports (Hirai *et al*., 2008; Masuda *et al*., 2002; Takabatake *et al*., 2007). RT-qPCR was performed using a Kapa SYBR Fast qPCR Kit (Kapa Biosystems, Woburn, MA, USA) with a Thermal Cycler Dice Real Time System II (Takara, Ohtsu, Japan) under the following conditions: 3 min at 94 °C for the first denaturation, followed by 40 cycles of 3 s at 94 °C for denaturation and 50 s at 60 °C for annealing and extension. After a final extension, a melting curve was performed from 70 to 95 °C to examine the specificity of the amplified product. The amount of actin was used for normalization of the amount of template cDNA.

Detection of CPRG mRNA

To prepare the DIG-labelled RNA probes for CPRGs, DNA fragments of the genes were RT-PCR amplified using the primers listed in Table S12 (see Supporting Information) and cloned into the pGEM-T easy vector. DIG-labelled RNA probes were transcribed *in vitro* from each plasmid after linearization by the appropriate restriction enzyme.

Total RNA was extracted from the tobacco tissues using the TriPure isolation reagent (Roche), and 3 μg of total RNA were loaded onto a 1.5% denaturing agarose gel and transferred onto a Hybond-N^+ membrane (GE Healthcare, Waukesha, WI, USA). The membrane was incubated with a DIG-labelled RNA probe in hybridization solution [7% sodium dodecylsulphate (SDS), 50% formamide, 5 × standard saline citrate (SSC), 0.1% *N*-lauroylsarcosine, 2% blocking reagent (Roche), 50 mM sodium phosphate, pH 7.0]. The detection of DIG signals was performed according to the manufacturer's instructions (Roche). The total RNA on the membrane was stained with methylene blue as a loading control.

 © 2013 BSPP AND JOHN WILEY & SONS LTD

ACKNOWLEDGEMENTS

This work was supported through funding from JSPS KAKENHI Grant #24780041.

REFERENCES

Arias, M.C., Luna, C., Rodriguez, M., Lenardon, S. and Taleisnik, E. (2005) *Sunflower chlorotic mottle virus* in compatible interactions with sunflower: ROS generation and antioxidant response. *Eur. J. Plant Pathol.* **113**, 223–232.

Babu, M., Gagarinova, A.G., Brandle, J.E. and Wang, A. (2008) Association of the transcriptional response of soybean plants with soybean mosaic virus systemic infection. *J. Gen. Virol.* **89**, 1069–1080.

Barajas-Lopez, J.D., Blanco, N.E. and Strand, A. (2013) Plastid-to-nucleus communication, signals controlling the running of the plant cell. *BBA-Mol. Cell. Res.* **1833**, 425–437.

Barrett, T., Troup, D.B., Wilhite, S.E., Ledoux, P., Rudnev, D., Evangelista, C., Kim, I.F., Soboleva, A., Tomashevsky, M. and Edgar, R. (2007) NCBI GEO: mining tens of millions of expression profiles—database and tools update. *Nucleic Acids Res.* **35**, D760–D765.

Brigneti, G., Voinnet, O., Li, W.X., Ji, L.H., Ding, S.W. and Baulcombe, D.C. (1998) Viral pathogenicity determinants are suppressors of transgene silencing in *Nicotiana benthamiana*. *EMBO J.* **17**, 6739–6746.

Dardick, C. (2007) Comparative expression profiling of *Nicotiana benthamiana* leaves systemically infected with three fruit tree viruses. *Mol. Plant–Microbe Interact.* **20**, 1004–1107.

Díaz-Vivancos, P., Clemente-Moreno, M.J., Rubio, M., Olmos, E., García, J.A., Martínez-Gómez, P. and Hernández, J.A. (2008) Alteration in the chloroplastic metabolism leads to ROS accumulation in pea plants in response to plum pox virus. *J. Exp. Bot.* **59**, 2147–2160.

Fitter, D.W., Martin, D.J., Copley, M.J., Scotland, R.W. and Langdale, J.A. (2002) GLK gene pairs regulate chloroplast development in diverse plant species. *Plant J.* **31**, 713–727.

Galvez-Valdivieso, G. and Mullineaux, P.M. (2010) The role of reactive oxygen species in signalling from chloroplasts to the nucleus. *Physiol. Plant.* **138**, 430–439.

García-Marcos, A., Pacheco, R., Martiáñez, J., González-Jara, P., Díaz-Ruíz, J.R. and Tenllado, F. (2009) Transcriptional changes and oxidative stress associated with the synergistic interaction between *Potato virus X* and *Potato virus Y* and their relationship with symptom expression. *Mol. Plant–Microbe Interact.* **22**, 1431–1444.

Gellért, A., Salánki, K., Náray-Szabó, G. and Balázs, E. (2006) Homology modelling and protein structure based functional analysis of five cucumovirus coat proteins. *J. Mol. Graph. Model.* **24**, 319–327.

Hanssen, I.M., van Esse, H.P., Ballester, A.R., Hogewoning, S.W., Parra, N.O., Paeleman, A., Lievens, B., Bovy, A.G. and Thomma, B.P. (2011) Differential tomato transcriptomic responses induced by pepino mosaic virus isolates with differential aggressiveness. *Plant Physiol.* **156**, 301–318.

Hirai, K., Kubota, K., Mochizuki, T., Tsuda, S. and Meshi, T. (2008) Antiviral RNA silencing is restricted to the marginal region of the dark green tissue in the mosaic leaves of tomato mosaic virus-infected tobacco plants. *J. Virol.* **82**, 3250–3260.

Ido, K., Ifuku, K., Yamamoto, Y., Ishihara, S., Murakami, A., Takabe, K., Miyake, C. and Sato, F. (2009) Knockdown of the PsbP protein does not prevent assembly of the dimeric PSII core complex but impairs accumulation of photosystem II supercomplexes in tobacco. *Biochim. Biophys. Acta*, **1787**, 873–881.

Ji, L.H. and Ding, S.W. (2001) The suppressor of transgene RNA silencing encoded by *Cucumber mosaic virus* interferes with salicylic acid-mediated virus resistance. *Mol. Plant–Microbe Interact.* **14**, 715–724.

Jia, M.A., Li, Y., Lei, L., Di, D., Miao, H. and Fan, Z. (2012) Alteration of gene expression profile in maize infected with a double-stranded RNA fijivirus associated with symptom development. *Mol. Plant Pathol.* **13**, 251–262.

Lehto, K., Tikkanen, M., Hiriart, J.B., Paakkarinen, V. and Aro, E.M. (2003) Depletion of the photosystem II core complex in mature tobacco leaves infected by the *flavum* strain of tobacco mosaic virus. *Mol. Plant–Microbe Interact.* **12**, 1135–1144.

Lewsey, M.G., Murphy, A.M., Maclean, D., Dalchau, N., Westwood, J.H., Macaulay, K., Bennett, M.H., Moulin, M., Hanke, D.E., Powell, G., Smith, A.G. and Carr, J.P. (2010) Disruption of two defensive signaling pathways by a viral RNA silencing suppressor. *Mol. Plant–Microbe Interact.* **23**, 835–845.

Liang, D.L., Yie, Y., Shi, D.J., Kang, L.Y. and Tien, P. (1998) The role of viral coat protein in the induction of mosaic symptoms in tobacco. *Sci. Chin. Ser. C, Life Sci.* **28**, 251–256.

Liu, S., He, X., Park, G., Josefsson, C. and Perry, K.L. (2002) A conserved capsid protein surface domain of *Cucumber mosaic virus* is essential for efficient aphid vector transmission. *J. Virol.* **76**, 9756–9762.

Loebenstein, G., Cohen, J., Shabtai, S., Coutts, R.H.A. and Wood, K.R. (1977) Distribution of cucumber mosaic virus in systemically infected tobacco leaves. *Virology*, **81**, 117–125.

Lu, J., Du, Z.X., Kong, J., Chen, L.N., Qiu, Y.H., Li, G.F., Meng, X.H. and Zhu, S.F. (2012) Transcriptome analysis of *Nicotiana tabacum* infected by *Cucumber mosaic virus* during systemic symptom development. *PLoS ONE*, **7**, e43447.

Luo, T., Luo, S., Araújo, W.L., Schlicke, H., Rothbart, M., Yu, J., Fan, T., Fernie, A.R., Grimm, B. and Luo, M. (2013) Virus-induced gene silencing of pea CHLI and CHLD affects tetrapyrrole biosynthesis, chloroplast development and the primary metabolic network. *Plant Physiol. Biochem.* **65**, 17–26.

Masuda, T., Fusada, N., Shiraishi, T., Kuroda, H., Awai, K., Shimada, H., Ohta, H. and Takamiya, K. (2002) Identification of two differentially regulated isoforms of protochlorophyllide oxidoreductase (POR) from tobacco revealed a wide variety of light- and development-dependent regulations of POR gene expression among angiosperms. *Photosynth. Res.* **74**, 165–172.

Mochizuki, T. and Ohki, S.T. (2011) Single amino acid substitutions at residue 129 in the coat protein of cucumber mosaic virus affect symptom expression and thylakoid structure. *Arch. Virol.* **156**, 881–886.

Mochizuki, T. and Ohki, S.T. (2012) *Cucumber mosaic virus*: viral genes as virulence determinants. *Mol. Plant Pathol.* **13**, 217–225.

Ohnishi, J., Hirai, K., Kanda, A., Usugi, T., Meshi, T. and Tsuda, S. (2009) The coat protein of *Tomato mosaic virus* L11Y is associated with virus-induced chlorosis on infected tobacco plants. *J. Gen. Plant Pathol.* **75**, 297–306.

Palukaitis, P. and García-Arenal, F. (2003) Cucumoviruses. *Adv. Virus Res.* **62**, 241–323.

Rizza, S., Conesa, A., Juarez, J., Catara, A., Navarro, L., Duran-Vila, N. and Ancillo, G. (2012) Microarray analysis of Etrog citron (*Citrus medica* L.) reveals changes in chloroplast, cell wall, peroxidase and symporter activities in response to viroid infection. *Mol. Plant Pathol.* **13**, 852–864.

Rodrigo, G., Carrera, J., Ruiz-Ferrer, V., del Toro, F.J., Llave, C., Voinnet, O. and Elena, S.F. (2012) A meta-analysis reveals the commonalities and differences in *Arabidopsis thaliana* response to different viral pathogens. *PLoS ONE*, **7**, e40526.

Rodríguez, M., Muñoz, N., Lenardon, S. and Lascano, R. (2012) The chlorotic symptom induced by *Sunflower chlorotic mottle virus* is associated with changes in redox-related gene expression and metabolites. *Plant Sci.* **196**, 107–116.

Saitoh, H., Fujiwara, M., Ohki, S.T. and Osaki, T. (1999) The coat protein gene is essential for the systemic infection of *Cucumber mosaic virus* in *Cucumis figarei* at high temperature. *Ann. Phytopathol. Soc. Jpn.* **65**, 248–253.

Salánki, K., Kiss, L., Gellért, A. and Balázs, E. (2011) Identification of a coat protein region of cucumber mosaic virus (CMV) essential for long-distance movement in cucumber. *Arch. Virol.* **156**, 2279–2283.

Satoh, K., Kondoh, H., Sasaya, T., Shimizu, T., Choi, I.R., Omura, T. and Kikuchi, S. (2010) Selective modification of rice (*Oryza sativa*) gene expression by rice stripe virus infection. *J. Gen. Virol.* **91**, 294–305.

Satoh, K., Shimizu, T., Kondoh, H., Hiraguri, A., Sasaya, T., Choi, I.R., Omura, T. and Kikuchi, S. (2011) Relationship between symptoms and gene expression induced by the infection of three strains of *Rice dwarf virus*. *PLoS ONE*, **22**, e18094.

Scholthof, K.B., Adkins, S., Czosnek, H., Palukaitis, P., Jacquot, E., Hohn, T., Hohn, B., Saunders, K., Candresse, T., Ahlquist, P., Hemenway, C. and Foster, G.D. (2011) Top 10 plant viruses in molecular plant pathology. *Mol. Plant Pathol.* **12**, 938–954.

Senthil, G., Liu, H., Puram, V.G., Clark, A., Stromberg, A. and Goodin, M.M. (2005) Specific and common changes in *Nicotiana benthamiana* gene expression in response to infection by enveloped viruses. *J. Gen. Virol.* **86**, 2615–2625.

Shimizu, T., Satoh, K., Kikuchi, S. and Omura, T. (2007) The repression of cell wall- and plastid-related genes and the induction of defense-related genes in rice plants infected with *Rice dwarf virus*. *Mol. Plant–Microbe Interact.* **20**, 247–254.

Shintaku, M.H., Zhang, L. and Palukaitis, P. (1992) A single amino acid substitution in the coat protein of *Cucumber mosaic virus* induces chlorosis in tobacco. *Plant Cell*, **4**, 751–757.

Song, X.S., Wang, Y.J., Mao, W.H., Shi, K., Zhou, Y.H., Nogués, S. and Yu, J.Q. (2009) Effects of cucumber mosaic virus infection on electron transport and antioxidant system in chloroplasts and mitochondria of cucumber and tomato leaves. *Physiol. Plant.* **135**, 246–257.

Sugiyama, M., Sato, H., Karasawa, A., Hase, S., Takahashi, H. and Ehara, Y. (2000) Characterization of symptom determinants in two mutants of cucumber mosaic virus Y strain, causing distinct mild green mosaic symptoms in tobacco. *Physiol. Mol. Plant Pathol.* **56**, 85–90.

Suzuki, M., Kuwata, S., Masuta, C. and Takanami, Y. (1995) Point mutations in the coat protein of cucumber mosaic virus affect symptom expression and virion accumulation in tobacco. *J. Gen. Virol.* **76**, 1791–1799.

Szilassy, D., Salánki, K. and Balázs, E. (1999) Stunting induced by cucumber mosaic cucumovirus-infected *Nicotiana glutinosa* is determined by a single amino acid residue in the coat protein. *Mol. Plant–Microbe Interact.* **12**, 1105–1113.

Takabatake, R., Ando, Y., Seo, S., Katou, S., Tsuda, S., Ohashi, Y. and Mitsuhara, I. (2007) MAP kinases function downstream of HSP90 and upstream of mitochondria in TMV resistance gene N-mediated hypersensitive cell death. *Plant Cell Physiol.* **48**, 498–510.

Takahashi, H. and Ehara, Y. (1992) Changes in the activity and the polypeptide composition of the oxygen-evolving complex in photosystem II of tobacco leaves infected with cucumber mosaic virus strain Y. *Mol. Plant–Microbe Interact.* **5**, 269–272.

Takahashi, H., Ehara, Y. and Hirano, H. (1991) A protein in the oxygen-evolving complex in the chloroplast is associated with symptom expression on tobacco leaves infected with cucumber mosaic virus strain Y. *Plant Mol. Biol.* **16**, 689–698.

Takahashi, H., Sugiyama, M., Sukamto, Karasawa, A., Hase, S. and Ehara, Y. (2000) A variant of *Cucumber mosaic virus* is restricted to local lesions in inoculated tobacco leaves with a hypersensitive response. *J. Gen. Plant Pathol.* **66**, 335–344.

Wang, C.M., Shi, D.J., Zhu, S.F., Tien, P. and Wei, N.S. (2000) Effects of *Cucumber mosaic virus* infection on photosynthetic activities of tobacco leaves and chloroplasts. *Acta Bot. Sin.* **42**, 388–392.

Waters, M.T. and Langdale, J.A. (2009) The making of a chloroplast. *EMBO J.* **28**, 2861–2873.

Waters, M.T., Wang, P., Korkaric, M., Capper, R.G., Saunders, N.J. and Langdale, J.A. (2009) GLK transcription factors coordinate expression of the photosynthetic apparatus in *Arabidopsis*. *Plant Cell*, **21**, 1109–1128.

Westwood, J.H., McCann, L., Naish, M., Dixon, H., Murphy, A.M., Stancombe, M.A., Bennett, M.H., Powell, G., Webb, A.A. and Carr, J.P. (2013) A viral RNA silencing suppressor interferes with abscisic acid-mediated signalling and induces drought tolerance in *Arabidopsis thaliana*. *Mol. Plant Pathol.* **14**, 158–170.

Whitham, S.A., Quan, S., Chang, H.-S., Cooper, B., Estes, B., Zhu, T., Wang, X. and Hou, Y.-M. (2003) Diverse RNA viruses elicit the expression of common sets of genes in susceptible *Arabidopsis thaliana* plants. *Plant J.* **33**, 271–283.

Yang, C., Guo, R., Jie, F., Nettleton, D., Peng, J., Carr, T., Yeakley, J., Fan, J. and Whitham, S. (2007) Spatial analysis of *Arabidopsis thaliana* gene expression in response to *Turnip mosaic virus* infection. *Mol. Plant–Microbe Interact.* **20**, 358–370.

Yi, X., Hargett, S.R., Frankel, L.K. and Bricker, T.M. (2009) The PsbP protein, but not the PsbQ protein, is required for normal thylakoid architecture in *Arabidopsis thaliana*. *FEBS Lett.* **583**, 2142–2147.

Yoon, J.Y., Chung, B.N. and Choi, S.K. (2011) High-temperature-mediated spontaneous mutations in the coat protein of cucumber mosaic virus in *Nicotiana tabacum*. *Arch. Virol.* **156**, 2173–2180.

SUPPORTING INFORMATION

Additional Supporting Information may be found in the online version of this article at the publisher's web-site:

Table S1 Up-regulated genes in pepo-infected pale green chlorosis tissue.

Table S2 Down-regulated genes in pepo-infected pale green chlorosis tissue.

Table S3 Up-regulated genes in 129A-infected pale green chlorosis tissue.

Table S4 Down-regulated genes in 129A-infected pale green chlorosis tissue.

Table S5 Up-regulated genes in 129Q-infected severe white chlorosis tissue.

Table S6 Down-regulated genes in 129Q-infected severe white chlorosis tissue.

Table S7 Number of individual differentially expressed genes (DEGs) annotated with each biological process gene ontology (GO) term in each *Cucumber mosaic virus* (CMV) sample.

Table S8 Number of identical differentially expressed genes (DEGs) annotated with each biological process gene ontology (GO) term common to all three *Cucumber mosaic virus* (CMV) samples.

Table S9 Gene responses to hormone signalling by *Cucumber mosaic virus* (CMV) infections.

Table S10 Gene responses related to transcriptional factors of *Cucumber mosaic virus* (CMV) infections.

Table S11 Primers used for the validation of microarray analysis by quantitative real-time polymerase chain reaction.

Table S12 Primers used for RNA probes to detect photosynthesis-related genes by Northern blot analysis.

 © 2013 BSPP AND JOHN WILEY & SONS LTD